arXiv:1409.7553v2 [physics.chem-ph] 28 Nov 2014

Molecular reordering processes on ice (0001) surfaces from long timescale simulations

Andreas Pedersen,[1,2] Kjartan T. Wikfeldt,[3,4] Leendertjan Karssemeijer,[5] Herma Cuppen,[5] and Hannes Jónsson[1,6]

[1)] *Faculty of Physical Sciences and Science Institute, University of Iceland, VR-III, 107 Reykjavík, Iceland*

[2)] *Integrated Systems Laboratory, ETH Zurich, 8092 Zurich, Switzerland*[a)]

[3)] *Science Institute, University of Iceland, VR-III, 107 Reykjavík, Iceland*

[4)] *NORDITA, AlbaNova University Center, S-10691 Stockholm, Sweden*

[5)] *Radboud University Nijmegen, Institute for Molecules and Materials, Heyendaalseweg 135, 6525 AJ Nijmegen, The Netherlands*

[6)] *Dept. of Applied Physics, Aalto University, Espoo, FI-00076, Finland*

We report results of long timescale adaptive kinetic Monte Carlo simulations aimed at identifying possible molecular reordering processes on both proton-disordered and ordered (Fletcher) basal plane (0001) surfaces of hexagonal ice. The simulations are based on a force field for flexible molecules and span a time interval of up to 50 μs at a temperature of 100 K, which represents a lower bound to the temperature range of Earth's atmosphere. Additional calculations using both density functional theory and an *ab initio* based polarizable potential function are performed to test and refine the force field predictions. Several distinct processes are found to occur readily even at this low temperature, including concerted reorientation (flipping) of neighboring surface molecules, which changes the pattern of dangling H-atoms, and the formation of interstitial defects by the downwards motion of upper-bilayer molecules. On the proton-disordered surface, one major surface roughening process is observed that significantly disrupts the crystalline structure. Despite much longer simulation time, such roughening processes are not observed on the highly ordered Fletcher surface which is energetically more stable because of smaller repulsive interaction between neighboring dangling H-atoms. However, a more localized process takes place on the Fletcher surface involving a surface molecule transiently leaving its lattice site. The flipping process provides a facile pathway of increasing proton-order and stabilizing the surface, supporting a predominantly Fletcher-like ordering of low-temperature ice surfaces, but our simulations also show that proton-disordered patches on the surface may induce significant local reconstructions. Further, a subset of the molecules on the Fletcher surface are susceptible to forming interstitial defects which might provide active sites for various chemical reactions in the atmosphere.

[a)]Electronic mail: andped10@gmail.com

I. INTRODUCTION

The surface of water ice plays a key role in atmospheric sciences. It moderates the temperature on Earth through reflection of sunlight, traps trace gases and catalyzes various chemical reactions that are inefficient in the gas phase. An important example of the latter is the production of active chlorine species that destroy ozone molecules in polar stratospheric regions[1]. The molecular-level structure and dynamics at ice surfaces are, however, difficult to investigate experimentally and a range of fundamental questions remains unanswered. At the same time, classical dynamics simulations are challenging because of the need for an accurate description of the molecular interactions and capturing processes that take place on a timescale that is very long compared with vibrational motion.

Ice Ih is the most common ice phase on Earth. In this phase, the oxygen atoms of the water molecules form a hexagonal tetrahedrally ordered lattice. The H_2O molecules can have a random orientation as long as the ice-rules are obeyed[2] – every H_2O donates and receives two hydrogen (H-) bonds and there is one H-atom between each nearest neighbor oxygen-oxygen pair. At moderate cooling below the freezing point, *i.e.*, from 273 K down to about 240 K, the ice surface is characterized by a disordered quasi-liquid layer, but the exact temperature at which this layer forms and how its thickness depends on temperature remains to be determined[3]. Nonetheless, timescales involved in this temperature range are within reach of conventional simulation techniques, and classical dynamics simulations using force fields have provided insights into such disordering and pre-melting phenomena[4–6]. At lower temperature, where polar stratospheric clouds form, below $\sim$ 200 K, the ice surface is more rigid but molecules in the top bilayer are still significantly more mobile than molecules in the crystal. Laser-induced thermal desorption measurements on isotopically substituted ice films have indicated a mean residence time in the range of 10^{-3} s to 10^{-6} s at 180-210 K before surface molecules diffuse into the crystal[7]. At even lower temperature, the surface structure and dynamics of ice is relevant for understanding chemical processes in polar mesospheric clouds that form at temperature down to around 140 K. Ice is also abundant in the interstellar medium where the temperature can be as low as $\sim$10 K. Although the majority of ice under such conditions is believed to be amorphous, observations suggest that also crystalline ice is present[8].

The molecular-level surface structure of ice at low temperature is still a subject of debate.

Low-energy electron diffraction (LEED)[9] and helium atom scattering experiments[10] has given strong support for a full-bilayer termination, *i.e.*, an intact surface bilayer, of the (0001) surface below 100 K although the LEED measurements at 90 K indicated sufficiently strong vibrational motions of the outermost molecules to render them undetectable[9]. If indeed basal plane ice surfaces do not reconstruct the question arises what the ordering is of dangling H-atoms (d-H) at the surface, *i.e.*, H-atoms that do not participate in H-bonds. The ice crystal is characterized by proton-disorder and if the disorder persisted on the surface these d-H would form a random pattern. This would lead to a large variety of adsorption sites on the surface, with a wide range in binding energy and activation energy for site-to-site hopping of water admolecules, reminiscent of the surface of an amorphous material[11]. However, several theoretical studies employing both empirical force fields[12] and density functional theory (DFT)[13,14] to determine minimum energy configurations of ice surfaces have shown that the ordered Fletcher surface[15] – where the d-H are arranged in a linearly striped pattern, see Fig. 1 – is the configuration with lowest surface energy since repulsive nearest neighbor interactions between d-H are minimized. The average number of nearest neighbor d-H,

$$C_{\mathrm{OH}} = \frac{1}{N_{\mathrm{OH}}} \sum_{i=1}^{N_{\mathrm{OH}}} c_i, \tag{1}$$

where N_{OH} is the total number of d-H and c_i is the number of nearest neighbor d-H surrounding molecule i, gives a simple and convenient measure of the average repulsive energy between d-H[13]. For the perfect Fletcher surface, C_{OH}=2.0, while C_{OH} increases with increasing disorder and a completely random arrangement gives $C_{\mathrm{OH}}\approx 3$[14]. Examples of both surface types are shown in Fig. 1, where C_{OH} for the disordered phase was determined to be 2.67. The Fletcher surface, is, however, entropically unfavorable[13,15], and a mosaic adopting an intermediate degree of linear order has been proposed as a lower free energy state[12].

Even though the detailed surface d-H morphology remains undetermined, it is known that the pattern has a large influence on the energetics of various types of surface defects[16,17] which may play an important role in determining the chemical reactivity of ice surfaces in the atmosphere as well as in interstellar space. However, obtaining structural and dynamical information on surface proton ordering, defect formation, and possible reconstructions of ice at low temperature is challenging for conventional simulation techniques due to the long timescales involved as compared with vibrational periods. The purpose of the present work

is to address this problem by applying the adaptive kinetic Monte Carlo (AKMC)[18] method to ice surfaces. Recently we demonstrated the ability of AKMC to simulate, without biasing the system in any way, the long timescale dynamics of a CO admolecule on the basal plane of ice[19]. In the present study, the long timescale dynamics of the pristine basal plane of ice is simulated using AKMC for both proton-ordered and disordered surfaces using the TIP4P/2005f[20] force field. Our AKMC simulations reveal several interesting reordering processes with sufficiently low energy barriers to occur readily on a μs timescale at 100 K. Interstitial defects can form on both disordered and Fletcher surfaces when a top half-bilayer molecule with a d-H reorients, shifts down and bonds to a second-bilayer molecule. On a proton-disordered surface we observe both a collective reorientation of three neighboring molecules in the surface bilayer, resulting in a stabilization of the surface due to lower repulsion between nearest neighbor d-H, and a surface roughening process that significantly disrupts the crystalline order in the top bilayer, yet still lowers the structural energy. Such a major reconstruction was not observed on the Fletcher surface, despite significantly longer simulation time, although one transient process occurred involving a molecule leaving its lattice site and forming a possible precursor state to a vacancy defect for around 10 ns before returning to its crystalline position. We then compare the energetics of the reordering processes observed using TIP4P/2005f to more advanced approaches, *i.e.*, DFT as well as the *ab initio*-based single-center multipole expansion (SCME) water model[21], to test and refine the force field predictions.

This paper is organized as follows. In the next section the ice surfaces and interaction potentials used in this study are described along with details of the AKMC method. We then present our results on both proton-disordered and ordered Fletcher surfaces and compare the force field predictions to more elaborate interaction models, and finally give concluding remarks in the final section.

II. METHODOLOGY

A. Hexagonal ice samples

To model and analyze the pristine ice Ih (0001) surface, two samples with different d-H patterns on the surface were constructed. Both samples contain 360 water molecules

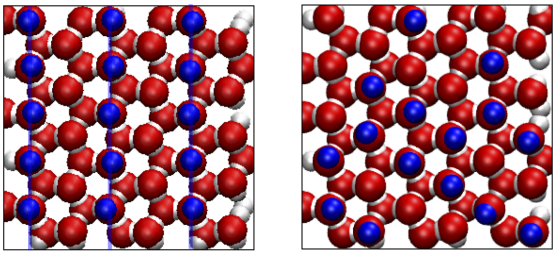


FIG. 1. (Color online) Ice Ih (0001) surfaces with a (left) Fletcher structure and a (right) proton-disordered structure. Dangling surface H-atoms, d-H, are colored blue. On the disordered surface there are local regions with a high density of nearest neighbor d-H while for the Fletcher surface all H-atoms are in a local environment with only two neighboring d-H.

arranged into 6 bilayers. The construction of each sample started from a hexagonal ice crystal with randomly generated H-bond network according to the method of Buch *et al.*[22]. The c-axis was chosen along the z-direction and periodic boundary conditions were applied in the x- and y-directions to mimic an infinite surface. The ionic and simulation cell degrees of freedom were then optimized using the TIP4P/2005f force field[20] under the constraint that the ratio between the side-lengths in x- and y-directions remained constant (a and c are allowed to vary). The resulting ratio between c and a is 1.738, which is 6.4% larger than the ratio for a perfect hcp lattice and 6.8% larger than the experimentally observed ratio for ice Ih[23]. For the energy-minimized structure, the lowest two bilayers were then frozen in the crystal configuration and the surface was created by adding a vacuum layer in the z-direction. This method generated an ice Ih substrate with a disordered d-H pattern. To create a Fletcher surface, the same method was applied, but with an initial crystal sample with a Fletcher-like H-bond pattern between two of the bilayers. The d-H patterns of both substrates are shown in Fig. 1. The calculated surface energy for the top bilayer is 8.40 meV/Å^2 and 9.13 meV/Å^2 for the Fletcher and disordered surfaces, respectively, calculated as

$$\gamma = \frac{1}{A}\left(\sum_{i=1}^{N=60} E_{\mathrm{b}}^{(i)} - N\,\langle E_{\mathrm{b}}\rangle\right) \tag{2}$$

where the sum runs over the binding energy E_{b} of all molecules in the top bilayer, $\langle E_{\mathrm{b}}\rangle$ is the cohesive energy of the crystal, 635 meV, and A is the surface area, 23.08 Å $\times$ 22.21 Å.

B. Adaptive kinetic Monte Carlo

To sample configuration space, the adaptive kinetic Monte Carlo method[18,24] was used as implemented in the EON software[25]. This involves sampling potential energy minima by traversing through saddle points (SPs) on the potential energy surface according to the kinetic Monte Carlo (KMC) algorithm. To locate SPs, the iterative minimum-mode following method was applied[26–28]. This method uses the lowest eigenvalue mode of the Hessian matrix which was, in this case, estimated by the Lanczos method[29,30]. The search for a SP starts by slightly displacing the system at random from its initial potential energy minimum, referred to here as reactant state. Then, the force component parallel to the minimum-mode is inverted and a climb on the potential energy surface up to a SP is conducted by applying an ordinary minimization algorithm. The two minima separated by the located SP, the reactant and product states, are determined by displacing the system along and in the opposite direction of the minimum-mode at the SP followed by minimization. Searches for SPs and minima were considered converged when the maximum force acting on any atom decreases below 1 meV/Å. Transition rates through the located SPs were estimated using Harmonic Transition State Theory (HTST):

$$k^{\mathrm{HTST}} = \nu \exp\left[-\frac{E_{\mathrm{SP}} - E_{\mathrm{R}}}{k_{\mathrm{b}}T}\right] \tag{3}$$

$$\nu = \frac{\prod_i^D \nu_{\mathrm{R},i}}{\prod_i^{D-1} \nu_{\mathrm{SP},i}}, \tag{4}$$

where E_{SP} is the energy of the SP, E_{R} is the energy of the reactant configuration, $\nu_{\mathrm{SP},i}$ and $\nu_{\mathrm{R},i}$ are the frequencies of the vibrational modes at the SP configuration excluding the unstable mode and the reactant configuration, respectively, and D is the number of degrees of freedom. For a given reactant state, a successful SP search that identifies a unique SP connecting to a product state is termed a transition and is entered into the event table of that state. When sufficiently many transitions for a reactant state have been found and the event table is considered to be complete enough, the simulation proceeds by picking one of the transitions at random with probability proportional to their relative rates. Time is then advanced by

$$\Delta t = -\frac{\ln \mu}{\sum_j k_j^{\mathrm{HTST}}}, \tag{5}$$

where μ is a random number on the interval $(0, 1]$ and j runs over all distinct transitions in the event table, and the system is moved to the product state.

The initial displacements to start the SP searches were made by rotating and translating one surface H_2O molecule chosen at random in the uppermost bilayer. The displacements were determined by values drawn from a Gaussian distributions having a standard deviation of 0.25 radians for the rotation and 0.25 Å for the displacement. The event table for each state was considered to be complete when a confidence level of 0.99 was obtained as defined by Xu *et al.*[31]. At this confidence level, an average of 438 (521) unique SPs were tabulated for each state visited on the disordered (Fletcher) surface, while the corresponding total numbers of located SPs were on average 1209 (1498). The success rate of the SP searches in finding low energy SPs connected to the initial state minimum was 57% (65%). To further enhance the sampling capability of AKMC, an automated coarse-graining procedure for grouping together states connected by fast transitions was applied[32,33]. The temperature was set to 100 K in the AKMC simulation, but the energy barrier and pre-exponential factor for each transition were saved and could in principle be used to simulate the system at other temperature within the HTST approximation.

C. Interaction potentials

In all the AKMC simulations, the inter- and intramolecular interactions were modeled with the TIP4P/2005f potential[20], which is a flexible version of the TIP4P/2005 potential[34]. The system is subject to periodic boundary conditions and all interactions are smoothly truncated at distances between 9 and 10 Å, based on the separation between the centers of mass of the molecules.

Empirical potentials such as TIP4P/2005f have been parametrized to fit various experimental data on extended phases such as liquids and/or crystals and are, therefore, not necessarily transferable to different environments such as an ice surface. To compare with previous DFT calculations on ice surfaces the vacancy formation energies for each of the 30 molecules in the upper half of the top bilayer for both the disordered and Fletcher surfaces were computed. One by one each surface molecule was removed and the vacancy defect surface relaxed. The vacancy formation energy is defined as the energy difference between the final relaxed defect surface and the initial defect-free surface. A broad distribution of

vacancy formation energies is found, ranging from 299 to 421 meV and from 179 to 422 meV for the Fletcher and disordered surfaces, respectively. The corresponding average energies are 365 and 311 meV, reflecting the larger stabilization of molecules on the Fletcher surface and thus larger vacancy formation energies. Both the averages and the magnitude of the variation are in rather good agreement with previous DFT calculations[16], where the PBE functional gave vacancy formation energies ranging from around 200 meV to 550 meV, and two dispersion-corrected functionals as well as the hybrid PBE0 functional gave consistent results (see Supplementary Material of ref.[16]). This suggests that TIP4P/2005f provides a reasonable description of the surface energetics. However, DFT predicted the existence of even higher energies than found here by TIP4P/2005f. This discrepancy can be easily understood since higher vacancy formation energies were found to correlate strongly with enhanced molecular dipole moments, but dipole polarizability is neglected in classical force fields such as TIP4P/2005f.

To further reinforce our conclusions presented below based on AKMC simulations employing TIP4P/2005f we performed additional calculations using DFT and a recent *ab initio*-based polarizable water potential, the single-center multipole expansion model (SCME)[21], on structures generated by the AKMC simulations. SCME describes water molecules as interacting static electric multipoles, with the expansion of the electric field going up to the hexadecapole, and many-body effects are treated by polarizable dipole and quadrupole moments. Apart from the rigorous description of the electrostatic interactions, SCME also includes dispersion coefficients from quantum chemistry calculations and a density-dependent short-range repulsion interaction. For DFT calculations a van der Waals density functional (optPBE-vdW[35]) was used to include non-local dispersion interactions which are important for a realistic description of ice[36]. This functional was shown to accurately describe the energetics of water clusters[35], and the density of ice Ih is predicted to within 2% accuracy compared to experiments while it overestimates the cohesive energy by 58 meV/H_2O, *i.e.*, around 10%[36]. SCME also predicts the equilibrium density of ice to be within 2% of experiments and, furthermore, accurately reproduces the experimental cohesive energy[21].

When evaluating DFT and SCME energies of the stable structures resulting from the AKMC simulations, the size of the cell was first rescaled, since neither optPBE-vdW nor SCME predict the same lattice parameters as TIP4P/2005f, and all ionic positions were then relaxed. The lattice parameters of SCME were reported in ref. 21 and those of optPBE-

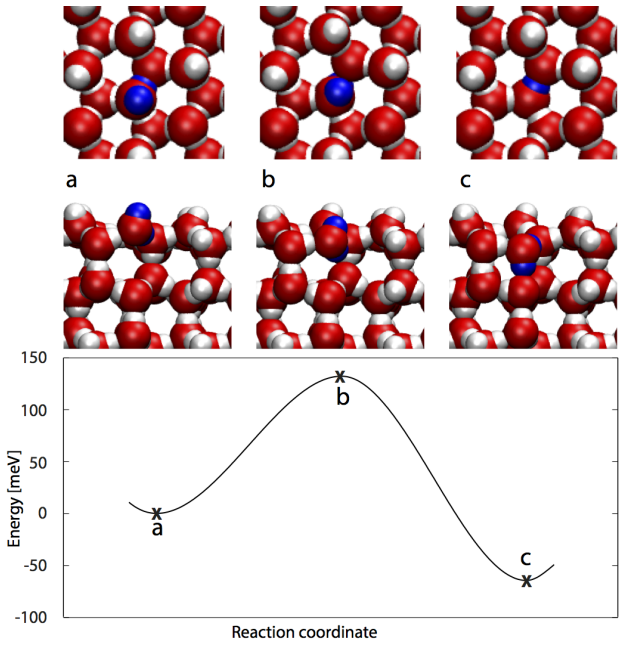


FIG. 2. (Color online) Formation of an interstitial defect on the proton-disordered surface where a top-half surface bilayer molecule shifts down into the surface. Upper row of insets are top-views and lower row are side-views. The energy of the pristine disordered surface defines the zero point on the energy scale. The H-atoms of the moving water molecule are colored blue. In this as well as following figures crosses mark computed energy of the stable and saddle point states found by AKMC, the continuous line is a guide to the eye and the insets only show the topmost bi-layer.

vdW in ref. 36. The DFT calculations were performed with the CP2K/Quickstep software[37], where the electronic structure is described with a dual Gaussian and plane-wave basis set. Core electrons were described by the Goedecker, Teter and Hutter (GTH) pseudopotentials[38], valence electrons were expanded in a molecularly-optimized polarized triple-ζ basis (TZVP-MOLOPT-GTH) and the cutoff energy of the auxiliary plane wave basis set was set to 340 Ry.

III. RESULTS

We now discuss the results of the AKMC simulations for the two models of the (0001) surface. Starting from both a disordered and a Fletcher surface the long timescale dynamics at 100 K was simulated. For the disordered surface, the simulation was terminated after a surface roughening process occurred at 0.11 μs when a total of 15330 unique transitions had

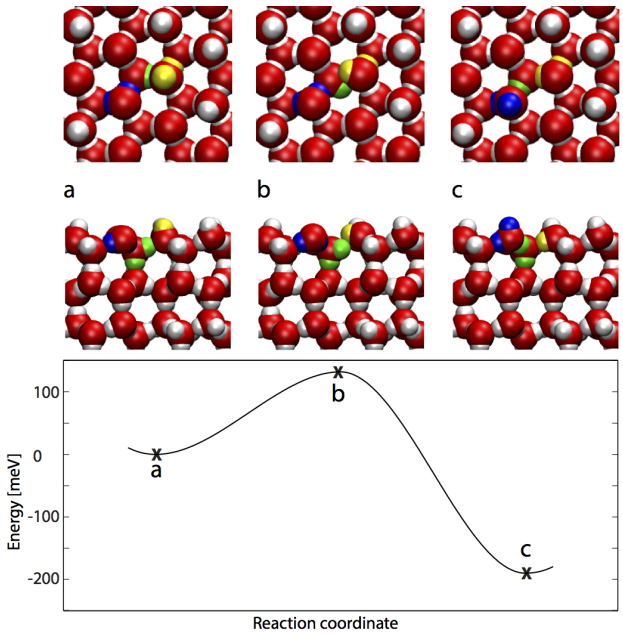


FIG. 3. (Color online) Concerted flipping of three molecules resulting in a reduced clustering of dangling H-atoms on the proton-disordered surface. Upper row of insets are top-views and lower row are side-views. Molecules participating in this reordering have differently colored H-atoms, and the energy of the pristine disordered surface defines the zero point on the energy scale.

been determined. The simulation of the Fletcher surface was continued up to 49.4 μs, at which time a total of 112536 unique transitions had been found.

A. Proton-disordered surface

Three types of reordering processes were observed on the disordered surface. Two of these processes have a strongly localized characater and involve the crossing of a single SP, while the third is a series of transitions resulting in a reordering of several surface water molecules and a roughening of the surface.

1. Interstitial formation

The simplest type of process observed was the creation of an interstitial defect. Although the event tables constructed from the SP searches contained several such transitions, only one was chosen as part of the time evolution of the system over the simulated time period

of 0.11 μs. This transition is depicted in Fig. 2 where the H-atoms of the affected molecule are colored blue. A surface water molecule with a d-H rotates in its molecular plane and shifts downwards by 1.55 Å to reach a configuration where it becomes an interstitial defect within the surface bilayer, forming a H-bond to a molecule in the top part of the second bilayer. The distance between the oxygen atoms in the newly formed H-bond is 2.83 Å, which is longer than the equilibrium distance of 2.73 Å in the crystal. In the final structure the number of d-H is decreased by one and the number of nearest neighbor d-H interactions decreases by four since the molecule was initially in a region with a cluster of d-H, see Fig. 2. For the transition to take place a barrier of 130 meV must be surpassed and the resulting change in energy is a lowering of 60 meV. The pre-exponential factor for this process was calculated to be $1.3 \cdot 10^{13}$ s^{-1}.

It might be expected that the molecule undergoing the transition to become an interstitial is in an energetically unfavorable geometry, particularly since it has four nearest neighbor d-H. However, while the average binding energy, E_{b}, of molecules in the upper part of the top bilayer is 490 meV before the interstitial formation, E_{b} of the affected molecule is 493 meV, close to the average. After becoming an interstitial, the binding energy of the molecule is significantly increased to 584 meV. On the other hand, the binding energy of the nearest neighbor molecules on the surface is only slightly increased, by at most by 8 meV due to the reduction in repulsive d-H interactions. A small destabilization of molecules surrounding the newly formed interstitial brings the total energy lowering down to 60 meV. The stabilization of the surface thus appears to be a consequence of the increased number of H-bonds formed when the initially d-H molecule rotates and shifts downwards to donate an H-bond to a second-bilayer molecule.

Calculated energy differences between reactant and product states of the interstitial formation process by DFT/optPBE-vdW and the polarizable SCME potential differ somewhat from the TIP4P/2005f value, as can be seen in Table I. SCME predicts qualitatively similar energetics with an energy lowering of 25 meV, while DFT predicts an energy increase of 64 meV. Since applying higher levels of theory for a system of this size would be prohibitively expensive, it can only be concluded at this point that the interstitial configuration is a local energy minimum with an energy close to the pristine surface. A more extensive discussion of the comparison between interaction potentials will be presented in section III D below.

2. Concerted reorientation

Another possible process on the disordered surface revealed by the AKMC simulation is a concerted reorientation of three molecules which shifts a d-H from one surface molecule to another. This process is analogous to the "relay" mechanism observed by Bishop *et al.*[6] in classical dynamics simulations using the NvdE six-site potential at 230 K, where it occurred on a ns timescale. Here, we find that it can occur also at 100 K on a μs timescale. Similarly as for the interstitial formation, several instances of this type of flipping process were found in the event tables constructed from the SP searches but only one was chosen as part of the simulated time evolution of the system. This transition is depicted in Fig. 3, where the affected molecules have H-atoms colored yellow, green and blue, respectively. In this reordering process a d-H of an upper-half bilayer surface molecule (yellow) in a dense d-H region rotates such that the d-H forms a new H-bond to a lower-half bilayer molecule (green). In the SP configuration the upper-half bilayer molecule has rotated by 120° while the second molecule has only partially rotated by around 60°. Going from the SP configuration to the final state, the lower-half bilayer molecule rotates another 60° to donate an H-bond to a second upper-half bilayer molecule (blue), which in turn rotates and becomes a molecule with a d-H. It can be seen that the number of nearest neighbor d-H interactions on the surface is reduced by two by swapping a d-H from a clustered d-H environment to a region with fewer d-H. Through this rearrangement the surface energy decreases by 190 meV by surpassing an energy barrier of 130 meV. The pre-exponential factor for this process is determined to be $1.1 \cdot 10^{14}$ s^{-1}.

The binding energy of all three molecules involved in the flipping process increases. The first molecule, initially with a d-H, is in an unstable geometry with E_b=438 meV, 52 meV below the average surface E_b. After the transition it is 481 meV, close to the average of 490 meV. The second molecule in the lower-half bilayer is stabilized by 30 meV, and the binding energy of the third molecule that rotates to become a d-H molecule increases from E_b=452 meV to E_b=483 meV, again moving closer to the average E_b. Since in the final configuration the number of d-H remains unchanged, the energy lowering is primarily due to the smaller number of repulsive nearest neighbor d-H interactions.

Table I shows that DFT/optPBE-vdW and SCME predict similar energetics for this process. The predicted stabilization is qualitatively consistent with TIP4P/2005f but more

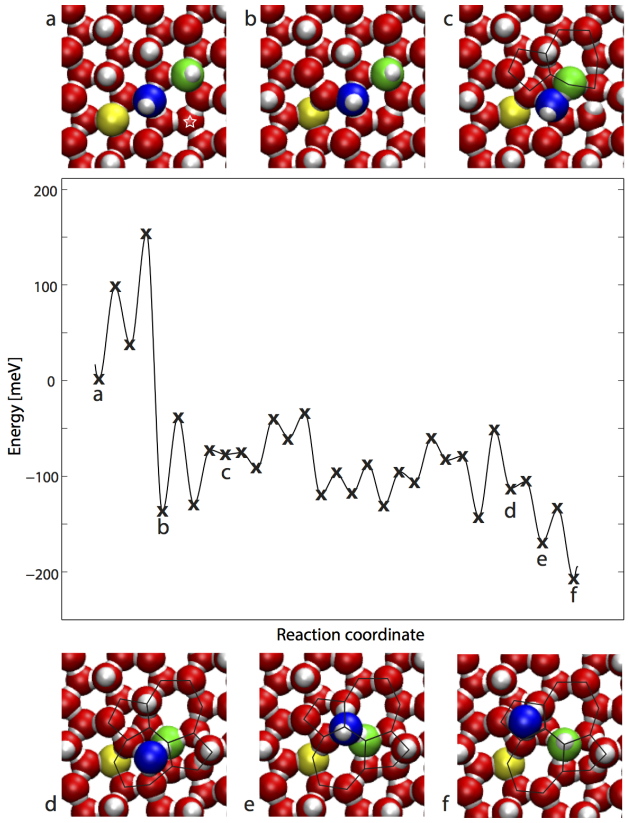


FIG. 4. (Color online) Roughening process on the proton-disordered surface. Insets are top-views. As the surface roughens it looses its perfect planar structure, a vacancy is formed in the surface bi-layer and an admolecule emerges on the surface. Oxygen atoms of the most active molecules are colored differently, and the energy of the initial disordered surface with one interstitial defect, marked by white star in panel a, defines the zero point of the energy scale.

exothermic by around 100 meV for SCME and by around 40 meV for DFT.

3. Surface roughening

The third structural change causing an energy lowering results from a series of 15 transitions starting from a surface with an interstitial defect, shown in Fig. 4, where the interstitial is marked by a white star. A distinct difference as compared with the previously discussed transitions is that this process causes a disruption of the hexagonal ordering of the O-atoms, leading to a large increase in structural entropy. The activation energy – the energy of the highest SP along this path – is 150 meV and the final reduction in energy amounts to 210 meV. The calculated values of the pre-exponential factor span a range from $5.4 \cdot 10^{12}$ s^{-1}

to $2.3 \cdot 10^{14}$ s^{-1}. In the first transition, a molecule from the upper-half surface bilayer, yellow in Fig. 4, shifts down by 1.2 Å while its H-bonded partner from the lower-half surface bilayer shifts up by 1.2 Å. We will refer to this as a "ripple" transition. Neither molecule has a d-H, and the only change in H-bond topology that takes place is that a third molecule from the second bilayer swaps its donating H-bond from the upward-moving to the downward-moving molecule. This destabilizes the surface slightly by 30 meV. Subsequently, a flipping transition occurs, analogous to the one discussed above, which reduces the number of nearest neighbor d-H interactions by two and results in a large drop in energy by around 172 meV and both transitions are visualized in Fig. 4, a→b. During the following two transitions, b→c, several concerted changes in H-bond connectivity take place between the initial interstitial defect and the position where the ripple transition took place. As a consequence of this reordering, the H-bonds within a hexagonal ring are stretched and two others rings change from being hexagonal to being pentagonal and heptagonal. This is similar to the Stone-Wales defect[39] observed in graphene, another hexagonal system. In graphene, and also in carbon nanotubes, the formation of these kind of defects are known to play a key role during the first steps of the melting transition[40]. Although such carbon-based systems are very different from hexagonal ice in many respects, it is interesting that similar defects are formed here in the AKMC simulation and it may indicate that they play a role in the premelting of hexagonal ice. In the following nine transitions, c→d, one molecule (blue) moves upwards and becomes an admolecule. The vacancy is accommodated in the surface by the formation of two additional five and seven membered rings around the green molecule in Fig. 4. The final two transitions, d→e→f, reveal a possible migration mechanism for the admolecule that formed. To reach the final state, f, the admolecule rotates and shifts to break the two donating H-bonds in state d and form two new H-bonds in state f. In the final state the number of d-H has decreased by one and the number of nearest neighbor d-H interactions by four compared to the initial state, a.

This process, which is composed of 15 distinct transitions, disrupts the crystalline order of the surface to a surprisingly large extent and it is important to check its feasibility when the molecular interactions are described using the alternative methods, DFT/optPBE-vdW and SCME. As seen in Table I, SCME predicts energetics similar to TIP4P/2005f with an energy lowering of 177 meV, while DFT also predicts a stabilization but of smaller magnitude, around 62 meV. This roughening of the hexagonal lattice thus appears to be a

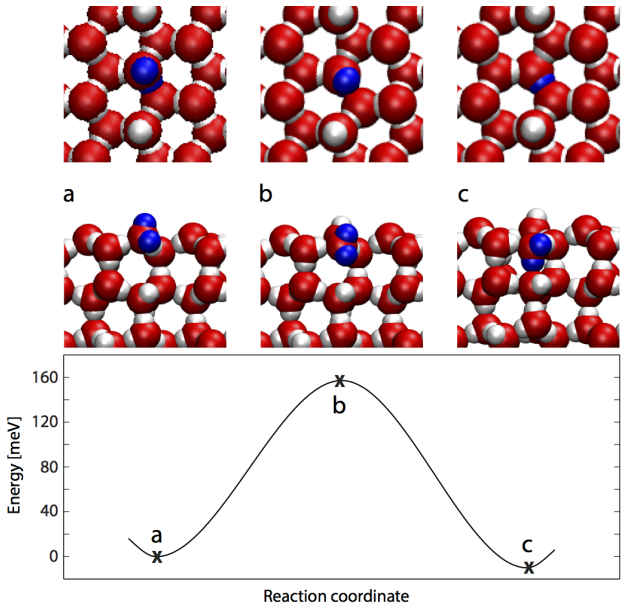


FIG. 5. (Color online) Formation of an interstitial defect on the perfect Fletcher surface where a top-half surface bilayer molecule shifts down into the surface. Upper row of insets are top-views and lower row are side-views. The energy of the pristine surface defines the zero point for the energy scale. The H-atoms of the moving water molecule are colored blue.

realistic process that might take place on proton-disordered ice surfaces at low temperature.

B. Fletcher surface

The AKMC simulation starting from a perfectly ordered Fletcher surface spanned a total of 49 μs and revealed two main types of processes. As in the case of the proton-disordered surface, interstitial defects can be created in single transitions, involving just one SP. Around 10% of the surface molecules shift frequently between the normal and interstitial positions. A process where one molecule temporarily leaves its lattice site, forming a possible precursor state to a vacancy defect on the surface, was also observed.

1. Interstitial formation

One representative example of an interstitial formation transition is shown in Fig. 5. For the process to take place, the system must overcome an energy barrier of 160 meV and the corresponding pre-exponential factor was calculated to be $3.0 \cdot 10^{13}$ s^{-1}. The barrier

for interstitial formation is thus 30 meV larger than for the disordered surface, the pre-exponential factor is smaller by a factor of 3.7 and the stabilization of the surface is only 10 meV. By breaking up one of the stripes of d-H and directing a d-H into the surface, the system decreases the number of d-H by one and the nearest neighbor d-H interactions by two. The mechanism for the creation of the interstitial defect is the same as for the disordered surface where a water molecule rotates in the molecular plane. In this transition the molecule shifts down by 1.38 Å which is slightly shorter than for the corresponding transition on the disordered surface. Similarly to the disordered surface, the binding energy of the displaced molecule increases from 489 meV, close to the average binding energy of upper half top bilayer molecules of 496 meV, to 555 meV. Other interstitial formation transitions with similar energetics take place during the simulation. Out of the 30 molecules in the upper half surface bilayer, three are particularly prone to becoming interstitial defects and they frequently switch between the normal and defect positions, spending a sizable fraction of the simulated time as defects. The average binding energy of these three molecules is 493 meV, close to the average E_{b}. Other factors than the binding energy, such as details of the ordering of H-bonds between the first and second bilayers, thus appear to determine the propensity of surface molecules to become interstitial defects.

Considering the previously assumed stability of the Fletcher surface[12–14], the slightly lower energy of the resulting interstitial defect surface compared to the pristine surface is interesting. We find that SCME predicts a very small stabilization, -5 meV, similar to TIP4P/2005f, while DFT/optPBE-vdW predicts a destabilization of 145 meV. Taking into account also the interstitial formation on the disordered surface, there thus appears to be a consistent trend where the TIP4P/2005f force field favors the formation of interstitial defects in order to reduce the number of d-H, while DFT disfavors it and the *ab initio*-based SCME potential gives results that are in between the other two.

2. Vacancy formation

The second type of process on the Fletcher surface can be viewed as the first series of transitions towards the formation of a surface vacancy, shown in Fig. 6. This process starts with the rate-limiting transition where a molecule (blue) rotates its d-H into the surface plane forming a H-bond to a neighboring upper-bilayer molecule with a dangling

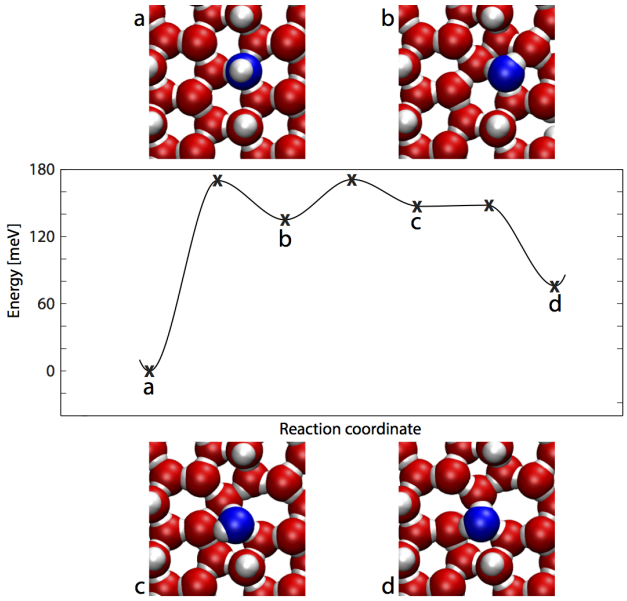


FIG. 6. (Color online) Possible first series of transitions in the formation of a vacancy defect on the Fletcher surface. Insets are top-views. The oxygen atom of the active molecule is colored blue. This process leads to a structure where one molecule has left its crystalline site, forming two heptamer and one pentamer rings, but in the AKMC simulation the molecule returned to its crystalline site after ∼10 ns.

oxygen lone-pair. The barrier for this transition is 170 meV, the pre-exponential factor is $3.6 \cdot 10^{13}$ s^{-1}, and the product state, b, is 135 meV less stable than the initial state. Through the following two transitions, b→c→d, the molecule leaves its lattice site and finds a more stable position which is, however, 75 meV less stable than the initial state, a. An analysis of the binding energy of the top bilayer molecules reveals that the major contribution to the destabilization is the less favorable position of the moving molecule which leaves a strongly bound site, E_b=503 meV, to enter a less favorable site, E_b=451 meV, in the final state. No further reordering transitions took place in the final state. Instead, the affected molecule returned to its initial crystalline position after around 10 ns.

For this process, the SCME and DFT/optPBE-vdW calculations predict a destabilization by 191 and 334 meV, respectively. Again, the more disordered nature of the final state leads to a larger energetic preference in DFT for the perfectly ordered Fletcher surface as compared to the TIP4P/2005f force field, with SCME giving results that are in between the other two.

TABLE I. Energy difference, $\Delta E \equiv E_{\text{product}} - E_{\text{reactant}}$, (in meV) between initial and final states of processes found by AKMC simulations using TIP4P/2005f, DFT/optPBE-vdW and SCME.

Process/Surface	TIP4P/2005f	DFT	SCME
Interstitial/disordered	-60	64	-25
Flip/disordered	-190	-230	-287
Roughening/disordered	-210	-62	-177
Interstitial/Fletcher	-10	145	-5
Vacancy/Fletcher	75	334	191

C. Comparison of disordered and Fletcher surfaces

The reordering processes discussed above are those selected by the AKMC algorithm from all the transitions identified by the SP searches for the proton-disordered and Fletcher surfaces. These transitions only constitute a small fraction of all the transitions entered in the event tables and additional information can be extracted by inspecting also the states which were not visited in the time evolution generated by the AKMC simulation. Figure 7 shows histograms of all transitions in the event tables that are likely to occur within specific timescales ordered by their relative energy change $\Delta E \equiv E_{\text{product}} - E_{\text{reactant}}$. To obtain a clear comparison between the disordered and Fletcher surfaces, we only considered processes with reactant states which are either perfectly crystalline or contain just a single interstitial defect. This gives 8 (5) possible initial states and 4056 (2635) transitions in total for the disordered (Fletcher) surface. The three classes of transitions shown in Fig. 7 correspond to those that can take place on a timescale τ of μs, ms or s. The timescale is obtained from the computed HTST rate as $\tau = 1/k^{\text{HTST}}$. These three classes contain 69 (26), 600 (315) and 1288 (877) transitions each for the disordered (Fletcher) surface.

The disordered surface contains a notably larger number of possible transitions that lower the energy than the Fletcher surface. Even on a $\sim\mu$s timescale, a range of processes that lower the energy can occur. The transitions with $\Delta E \approx$-180 meV correspond to flipping transitions and are similar to the one discussed in section III A and occur on several of the 8 unique initial states of the disordered surface chosen for this analysis. The roughening process shown in Fig. 6 is not included here since it involves a series of transitions. In contrast, $\sim\mu$s processes on the Fletcher surface all increase the energy. A closer inspection

of the processes marked by black bars in Fig. 7, lower panel, reveals that they involve small perturbations to the surface H-bonds with small molecular displacements. The processes accessible on a longer timescale on the Fletcher surface and involve small energy changes are dominated by interstitial formation transitions as well as ripple transitions.

This comparison of possible transitions found by the SP searches in AKMC, shown in Fig. 7, demonstrates that the surface order present on the Fletcher surface greatly reduces the number of molecular reordering processes that lower the energy. Thus, even though the difference in surface energy between the disordered and Fletcher surfaces is only around 0.73 meV/Å^2, or about 9%, the linear ordering of d-H on the Fletcher surface has a large effect on the energetics of possible reordering processes.

D. Comparison of interaction potentials

The AKMC simulations using the TIP4P/2005f force field identified several processes that can take place on the basal plane surface of ice Ih at low temperature, and the viability of these has been tested using more elaborate approaches, *i.e.*, DFT/optPBE-vdW and the SCME *ab initio*-based model. Some conclusions can be drawn from this comparison. Firstly, it is worth highlighting that the product states found by AKMC with the TIP4P/2005f force field are also stable local energy minima when DFT/optPBE-vdW and the SCME potential are used to compute interatomic forces. After rescaling the simulation cell to conform to the DFT/optPBE-vdW or SCME equilibrium lattice constants and relaxing the atomic coordinates, it is found that the geometrical changes occurring in the transitions found by AKMC are similar for the three different descriptions of the molecular interactions. For instance, in the two interstitial formation processes discussed above, on the disordered and Fletcher surfaces, TIP4P/2005f predicts that the affected molecule shifts downwards by 1.55 Å and 1.38 Å, respectively. The corresponding numbers from DFT/optPBE-vdW are 1.49 Å and 1.33 Å while SCME predicts 1.60 Å and 1.38 Å. This adds confidence in the TIP4P/2005f force field as a reliable model for the description of the interaction between water molecules at ice surfaces and suggests that the reordering processes discovered in the AKMC simulations are realistic.

Some deviations are nonetheless seen in the energetics. In the case of the concerted flipping process on the disordered surface, there is good qualitative agreement between

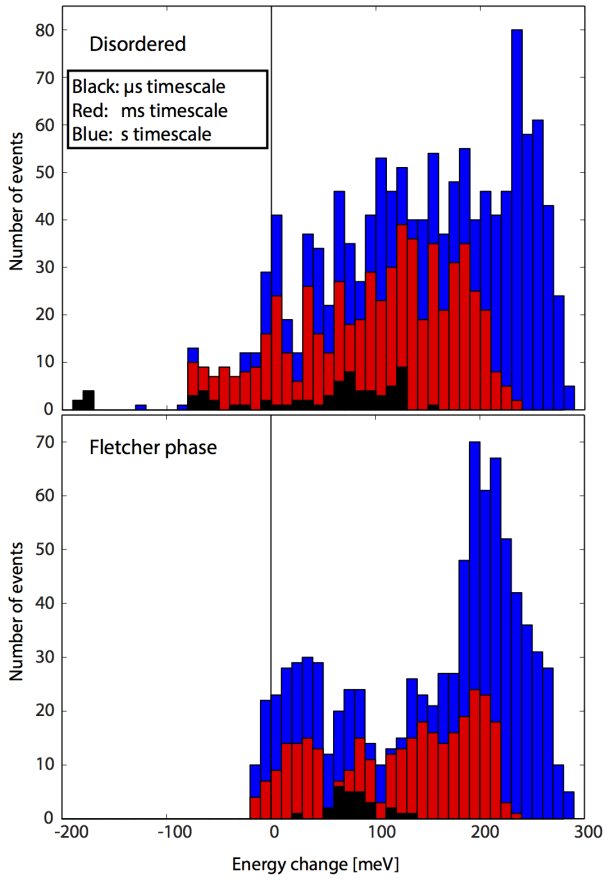


FIG. 7. (Color online) Histograms of energy changes for transitions found by AKMC extracted from all transition tables for the proton-disordered and Fletcher surfaces. Three classes of transitions are shown corresponding to μs, ms and s timescales, respectively. The only transitions included are those that can take place from pristine surfaces with 15 d-H or a surface characterized by a single interstitial defect.

TIP4P/2005f, DFT/optPBE-vdW and SCME, all predicting a stabilization of the surface by 190-290 meV, see Table I. The energetics of this process is dominated by the electrostatic repulsion between dangling H-atoms on the surface. Qualitative disagreement arises in the case of the interstitial formation process on both the disordered and the Fletcher phase surfaces, where TIP4P/2005f and SCME predict a stabilization while DFT/optPBE-vdW gives a higher energy for the less ordered final state. In these final states the local environment around the interstitial molecule is of higher density than in the ice crystal; the H-bonds are more bent compared to the crystal and dispersion (van der Waals) interactions become stronger. The energetics are dictated by a balance between electrostatic and dis-

persion interactions and the interstitial geometry thus presents a challenge to interaction potentials for water. *A priori* it cannot be assumed that DFT/optPBE-vdW is significantly more accurate than TIP4P/2005f or SCME, especially considering that it overestimates the cohesive energy of the ice crystal by 58 meV/H_2O compared to experiment[36]. In order to predict the abundance of interstitial defects on basal plane ice surfaces, it will be important to obtain more accurate theoretical values for these energy differences.

All methods applied here agree in that the surface roughening process lowers the interaction energy, with close agreement between TIP4P/2005f, -200 meV, and SCME, -180 meV, while DFT/optPBE-vdW predicts weaker stabilization, -60 meV. Since the final state after the roughening process is characterized by a disordered, non-crystalline structure it appears likely that the weaker stabilization of DFT/optPBE-vdW derives from a different balance between electrostatic and dispersion interactions. The same holds true for the vacancy formation process on the Fletcher surface, where DFT/optPBE-vdW predicts the largest destabilization of the final state, which is characterized by a local disruption of the crystalline structure.

IV. CONCLUSIONS

We have carried out AKMC simulations, which are free from preconceived notions of possible transition mechanisms, to shed light on possible molecular reordering processes of ice surfaces in the cooler regions of Earth's atmosphere. Structural and dynamical details of such processes are of fundamental importance to a range of atmospheric chemical reactions, but previous experimental and theoretical studies of ice surfaces have left many questions unanswered. The results presented here demonstrate how the AKMC method can be used to investigate long timescale evolution of complex systems such as the basal plane ice surface, without the need to apply biasing potentials or to increase temperature. In particular, through automated saddle point searches, AKMC can reveal new and unexpected reordering mechanisms.

Our observation of a series of transitions that lead to a large distortion of the hexagonal lattice of O-atoms at the proton-disordered surface is difficult to reconcile with existing helium atom scattering experimental data[10] which indicate a smooth basal plane ice surface at 90 K. The initial proton-disordered surface, constructed with a commonly used method

for generating proton-disordered ice simulation cells, was metastable with respect to a disordering reconstruction which is hardly reversible due to the associated increase in structural entropy. Further, the flipping process that occurred on the proton-disordered surface provides a possible low-barrier exothermic pathway to increase proton order. Hence it appears unlikely that completely proton-disordered surfaces are representative models of real ice surfaces at low temperature. Although by no means conclusive, the lack of any processes leading to significant distortions of the lattice on the Fletcher surface, despite ∼500 times longer simulation time than for the proton-disordered surface, suggests that proton-order inhibits such processes at low temperature. Furthermore, our analysis of the event tables constructed by AKMC showed that the Fletcher surface is significantly more robust against local reordering transitions than the disordered substrate. In combination with the above mentioned experiments, our simulation results, therefore, suggest that the surface is to a large extent stabilized by stripes of dangling H-atoms as suggested by Fletcher[15]. This is particularly interesting when considering the relatively small difference, less than 9%, in the energy of the two surfaces. Further work, however, will be required to reveal in more detail what type of patterns of dangling H-atoms might emerge and how they depend on temperature.

Our results also highlight the importance of carefully considering the surface proton order in simulation studies of ice, *e.g.*, when investigating atmospheric chemical reactions. Using proton-disordered surfaces with a large amount of repulsive interactions between dangling H-atoms may lead to unrealistic predictions of the energetics and reaction pathways.

On the other hand, the formation of proton-disordered patches on largely proton-ordered ice surfaces might be considered as rare events that can occur locally. Previous experimental measurements may have been insensitive to the type of roughening of crystalline order that we observe on the proton-disordered surface, but its possible importance for the chemical reactivity of ice surfaces motivates further experimental efforts to characterize in more detail the surface structure of ice at low temperature.

Simpler reordering processes are observed on the ordered Fletcher surface over a time interval of 49 μs, where several molecules frequently rotate around their molecular axis and shift into the surface to become interstitial defects. Some of the surface molecules are particularly susceptible to these processes and spend a significant portion of the simulated time in the defect geometry. Moreover, our observation of a transient process on the Fletcher

surface lasting about 10 ns which leads to a possible precursor state to a surface vacancy defect, suggests that surface vacancies may form on a μs timescale even at low temperature, *i.e.*, around 100 K. Future experimental and theoretical work would be required to quantify the propensity of defects and elucidating how they affect the chemical reactivity of ice surfaces.

A. Acknowledgement

The authors would like to thank Dr. J-C. Berthet for helpful discussions. This work was supported by the Icelandic Research Fund and the University of Iceland Research Fund. K.T.W. is supported by the Icelandic Research Fund through Grant No. 120044042. L.J.K and H.M.C are funded by the European Research Council (ERC-2010-StG, Grant Agreement no. 259510-KISMOL) and H.M.C. thanks The Netherlands Organization for Scientific Research (NWO) (VIDI 700.10.427). A.P. thanks the COST Action CM0805 for enabling a research visit.

REFERENCES

[1]T. Bartels-Rausch, V. Bergeron, J. H. E. Cartwright, R. Escribano, J. L. Finney, H. Grothe, P. J. Gutiérrez, J. Haapala, W. F. Kuhs, J. B. C. Pettersson, *et al.*, "Ice structures, patterns, and processes: a view across the icefields," Rev. Mod. Phys. **84**, 885 (2012).

[2]J. D. Bernal and R. H. Fowler, "A Theory of Water and Ionic Solution, with Particular Reference to Hydrogen and Hydroxyl Ions," J. Chem. Phys. **1**, 515 (1933).

[3]Y. Li and G. A. Somorjai, "Surface premelting of ice," J. Phys. Chem. C. **111**, 9631–9637 (2007).

[4]G.-J. Kroes, "Surface melting of the (0001) face of tip4p ice," Surf. Sci. **275**, 365–382 (1992).

[5]K. Bolton and J. B. C. Pettersson, "A Molecular Dynamics Study of the Long-Time Ice Ih Surface Dynamics," J. Phys. Chem. B. **104**, 1590–1595 (2000).

[6]C. L. Bishop, D. Pan, L. M. Liu, G. A. Tribello, A. Michaelides, E. G. Wang, and B. Slater, "On thin ice: surface order and disorder during pre-melting," Faraday Discuss. **141**, 277 (2008).

[7]D. Brown and S. George, "Surface and bulk diffusion of h218o on single-crystal h216o ice multilayers," J. Phys. Chem. **100**, 15460–15469 (1996).

[8]M. Maldoni, M. Egan, R. Smith, G. Robinson, and C. Wright, "Crystalline water ice in oh32. 8–0.3," Mon. Not. R. Astron. Soc. **345**, 912–922 (2003).

[9]N. Materer, U. Starke, A. Barbieri, M. Van Hove, G. Somorjai, G.-J. Kroes, and C. Minot, "Molecular surface structure of ice (0001): dynamical low-energy electron diffraction, total-energy calculations and molecular dynamics simulations," Surf. Sci. **381**, 190–210 (1997).

[10]A. Glebov, A. Graham, A. Menzel, J. Toennies, and P. Senet, "A helium atom scattering study of the structure and phonon dynamics of the ice surface," J. Chem. Phys. **112**, 11011–11022 (2000).

[11]E. R. Batista and H. Jónsson, "Diffusion and Island formation on the ice Ih basal plane surface," Comput. Mater. Sci. **20**, 325–336 (2001).

[12]V. Buch, H. Groenzin, I. Li, M. J. Shultz, and E. Tosatti, "Proton order in the ice crystal surface," P. Natl. Acad. Sci. USA **105**, 5969–5974 (2008).

[13]D. Pan, L.-M. Liu, G. Tribello, B. Slater, A. Michaelides, and E. G. Wang, "Surface Energy and Surface Proton Order of Ice Ih," Phys. Rev. Lett. **101**, 155703 (2008).

[14]D. Pan, L.-M. Liu, G. A. Tribello, B. Slater, A. Michaelides, and E. G. Wang, "Surface energy and surface proton order of the ice Ih basal and prism surfaces," J. Phys.: Condens. Matter. **22**, 074209 (2010).

[15]N. H. Fletcher, "Reconstruction of ice crystal surfaces at low temperatures," Philosophical Magazine B **66**, 109–115 (1992).

[16]M. Watkins, D. Pan, E. Wang, A. Michaelides, J. VandeVondele, and B. Slater, "Large variation of vacancy formation energies in the surface of crystalline ice," Nature Materials **10**, 794–798 (2011).

[17]M. Watkins, J. VandeVondele, and B. Slater, "Point defects at the ice (0001) surface," P. Natl. Acad. Sci. USA **107**, 12429–12434 (2010).

[18]G. G. Henkelman and H. Jónsson, "Long time scale kinetic Monte Carlo simulations without lattice approximation and predefined event table," J. Chem. Phys. **115**, 9657–9666 (2001).

[19]L. Karssemeijer, A. Pedersen, H. Jónsson, and H. M. Cuppen, "Long-timescale simulations of diffusion in molecular solids," Phys. Chem. Chem. Phys. **14**, 10844 (2012).

[20]M. A. González and J. L. F. Abascal, "A flexible model for water based on TIP4P/2005," J. Chem. Phys. **135**, 224516 (2011).

[21]K. T. Wikfeldt, E. R. Batista, F. D. Vila, and H. Jónsson, "A transferable h2o interaction potential based on a single center multipole expansion: Scme," Phys. Chem. Chem. Phys. **15**, 16542–16556 (2013).

[22]V. Buch, P. Sandler, and J. Sadlej, "Simulations of H2O Solid, Liquid, and Clusters, with an Emphasis on Ferroelectric Ordering Transition in Hexagonal Ice," J. Phys. Chem. B. **102**, 8641–8653 (1998).

[23]K. Röttger, A. Endriss, J. Ihringer, S. Doyle, and W. F. Kuhs, "Lattice constants and thermal expansion of H2O and D2O Ice I hbetween 10 and 265K and Addendum," Acta Crystallographica Section B Structural Science **68**, 91–91 (2012).

[24]A. Pedersen and H. Jónsson, "Distributed implementation of the adaptive kinetic Monte Carlo method," Mat. Comput. Sim. **80**, 1487–1498 (2010).

[25]S. T. Chill, M. Welborn, R. Terrell, L. Zhang, J.-C. Berthet, A. Pedersen, H. Jonsson, and G. Henkelman, "Eon: software for long time simulations of atomic scale systems," Modelling Simul. Mater. Sci. Eng. **22**, 055002 (2014).

[26]G. Henkelman and H. Jónsson, "A dimer method for finding saddle points on high dimensional potential surfaces using only first derivatives," J. Chem. Phys. **111**, 7010–7022 (1999).

[27]R. A. Olsen, G. J. Kroes, G. Henkelman, A. Arnaldsson, and H. Jónsson, "Comparison of methods for finding saddle points without knowledge of the final states," J. Chem. Phys. **121**, 9776–9792 (2004).

[28]A. Pedersen, S. F. Hafstein, and H. Jónsson, "Efficient Sampling of Saddle Points with the Minimum-Mode Following Method," SIAM Journal on Scientific Computing **33**, 633 (2011).

[29]J. Tennyson, "The calculation of the vibration-rotation energies of triatomic molecules using scattering coordinates," Comput. Phys. Rep. **4**, 1–36 (1986).

[30]R. Malek and N. Mousseau, "Dynamics of lennard-jones clusters A characterization of the activation-relaxation technique," Phys. Rev. E. **62**, 7723–7728 (2000).

[31]L. Xu and G. G. Henkelman, "Adaptive kinetic Monte Carlo for first-principles accelerated dynamics," J. Chem. Phys. **129**, 114104 (2008).

[32]A. Pedersen, J. C. Berthet, and H. Jónsson, "Simulated annealing with coarse graining and distributed computing," Appl. Parallel and Scientific Computing , 34–44 (2012).

[33]H. Jónsson, "Simulation of surface processes," P. Natl. Acad. Sci. USA **108**, 944–949 (2011).

[34]J. L. F. Abascal and C. Vega, "A general purpose model for the condensed phases of water: TIP4P/2005," J. Chem. Phys. **123**, 234505 (2005).

[35]J. Klimeš, D. R. Bowler, and A. Michaelides, "Chemical accuracy for the van der waals density functional," J. Phys.: Cond. Matter **22**, 022201 (2010).

[36]B. Santra, J. Klimeš, A. Tkatchenko, D. Alfè, B. Slater, A. Michaelides, R. Car, and M. Scheffler, "On the accuracy of van der waals inclusive density-functional theory exchange-correlation functionals for ice at ambient and high pressures," J. Chem. Phys **139**, 154702 (2013).

[37]J. VandeVondele, M. Krack, F. Mohamed, M. Parrinello, T. Chassaing, and J. Hutter, "Quickstep: Fast and accurate density functional calculations using a mixed gaussian and plane waves approach," Comput. Phys. Comm. **167**, 103–128 (2005).

[38]S. Goedecker, M. Teter, and J. Hutter, "Separable dual-space gaussian pseudopotentials," Phys. Rev. B. **54**, 1703 (1996).

[39]A. J. Stone and D. J. Wales, "Theoretical studies of icosahedral c_{60} and some related species," Chem. Phys. Lett. **128**, 501–503 (1986).

[40]K. V. Zakharchenko, A. Fasolino, J. H. Los, and M. I. Katsnelson, "Melting of graphene: from two to one dimension," J. Phys.: Condens. Matter. **23**, 202202 (2011).